Accurate Investigation of Coupled Plasmonic Resonances in a Chain of Silver Nanowires

Nadiia P. Stognii [1,2], Nataliya K. Sakhnenko [1]

[1] Department of Higher Mathematics, Kharkiv National University of Radio Electronics, Kharkiv, Ukraine

[2] Laboratory of Micro and Nano Optics, Institute of Radio Physics and Electronics NASU
Kharkiv, Ukraine
e-mail: nstognii@gmail.com

Abstract— **This paper presents investigation of plasmonic properties of coupled metal nanowires arranged to form a finite linear chain. Coupled plasmon resonances of such structures embedded into dielectrics with different dielectric permittivity are studied. The main goals of the paper are to validate true potential of a plasmon nanowire-based structure in sensing applications and to reveal optimized configurations with narrowband plasmonic resonances and enhanced sensitivity.**

Keywords—**Plasma; localised surface plasmons; plasmon resonances; eigenfrequency; linear chain.**

I. INTRODUCTION

In recent years nanooptics and nanotechnology have been considered as a priority in science and technology. The development of nanofabrication together with new achievements in nanotechnology are stimulating the interest in the propagation and scattering of electromagnetic waves in metallic nanostructures.

Plasmonic structures and their optical fields have been the subject of significant interest in recent years. Using resonators composed of negative permittivity materials such as plasma can form the basis of effective small-size antenna elements [1]. Plasmonic structures of different shapes (nanowires, nanorods, nanospheres, nanoshells) are provided by various fabrication techniques. The silver nanowire structure is a candidate for key components in future ultracompact photonic devises [2, 3]. It can be considered as a plasmon biosensor to monitor tiny biomolecular concentrations [4], as a novel modulator to control the intensity of the transmitted surface plasmon polaritons through a nanowire array [5] and as a nanolaser [6, 7]. Plasmons have been also explored for their potential in single molecule detection and biomolecular interaction studies.

Theoretical studies of modern nanoscale devices require highly accurate simulations that are complicated by the open nature of the structures. It leads to very long simulation times if using purely numerical approaches. Alternatively, analytical solutions can give conceptually informative solutions and provide valuable insight but they can be obtained, as a rule, only in very simple canonical cases. In this paper, we use numerical-analytical schemes combining analytical and numerical solutions together to qualitatively reveal the underlying physical principles involved.

II. MATHEMATICAL BACKGROUND: FORMULATION AND SOLUTION

In this paper, we consider coupled localized surface plasmons (SPs) in nanowires forming a finite linear chain (Fig. 1). In computations, we assume that the radius of each wire is $a = 20$ nm and the separation distance between them is d . The metal refractive index n_p is taken from the experimental data of Jonson and Christie [3] for bulk silver, permittivity of outer space is n_1 , and time dependence is $e^{i\omega t}$.

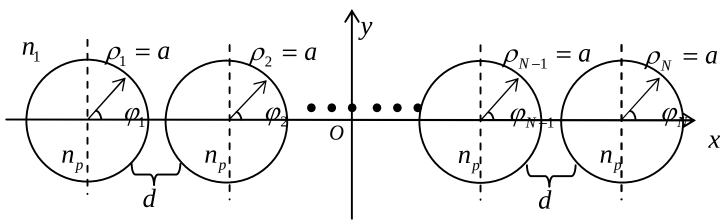

Fig. 1. Schematic diagram of the cross-section of the considered structure: a finite linear chain of N nanowires.

To characterize the fields, the local systems of polar coordinates associated with each wire are introduced. The solution is presented in the form of sum of the series in local azimuth angles,

$$H_m(\rho_m,\varphi_m) = \sum_{s=-\infty}^{+\infty} A_s^m J_s(k_p\rho_m) e^{is\varphi_m}, \; m = 1,...,N, \qquad (1)$$

$$H(\rho,\varphi) = \sum_{m=1}^{N}\sum_{s=-\infty}^{+\infty} \bar{A}_s^m H_s^{(2)}(k\rho) e^{is\varphi}, \qquad (2)$$

Here $k = \omega \cdot c^{-1}$, c is light velocity in a vacuum, N is number of nanowires in chain, equation (1) presents internal field for each particular wire, while (2) characterizes external field, global polar coordinates (ρ,φ) are associated with the (x, y) the Cartesian system.

The coefficients A_s and $\bar{A}_s$ are found from the boundary conditions requiring the continuity of the tangential components of the total electric and magnetic fields at each surface. Using the addition theorem for the Bessel functions, we arrive at an infinite set of algebraic equations that can be truncated in order to provide a controlled numerical precision.

The solution of the plane wave scattering problem for a linear chain of silver nanowires was obtained in [4]. In this paper, we concentrate on deriving the formulas for eigenfrequencies, i.e. we solve the eigenvalue problem with zero incident field. Generally, the plasmonic eigenfrequencies of the linear chain are roots of the *N*-block matrix determinant equation. With growing of N the solution of the equation becomes more complicated. However, the problem can be simplified using the following observations. The structure under consideration has two axes of symmetry that causes four families of coupled plasmon natural modes. They can be classified as EE SPs with field patterns symmetrical (even) with respect to the x and the y axes, EO with field patterns symmetrical (even) with respect to the x -axis and antisymmetrical (odd) with respect to the y -axis), similarly, OE (x –odd; y -even), OO (x –odd; y -odd). Here we follow classification proposed in [9,11,12] for eigenmodes in thin-disk photonic molecules.

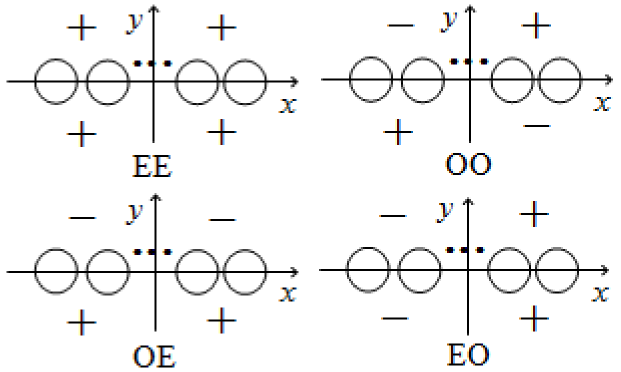

Fig. 2. Four classes of symmetry of the natural-mode field: EE (x -even, y -even), OO (x -odd, y -odd), OE (x -odd, y -even), EO (x -even, y -odd).

Fig. 2 shows the classification scheme of possible SP mode symmetry classes in a finite linear chain. For each symmetry class the eigenfrequency equation can be simplified and written in the following form:

EE (x -even, y -even)

$$x_m^{(p)} + J_m(ka)\sum_{j=1}^{N/2}\sum_{s=0}^{\infty}\mu_s x_s^{(j)} U_s W_{ms}^{(p,j)} + 2J_m(ka)\sum_{s=0}^{\infty}\mu_s x_{2s}^{(N+1)/2} U_{2s} W_{m,2s}^{(p,(N+1)/2)} = 0, \tag{3}$$

OE (x –odd; y -even)

$$x_m^{(p)} - J_m(ka)\sum_{j=1}^{N/2}\sum_{s=1}^{\infty} x_s^{(j)} U_s W_{ms}^{(p,j)} + 2J_m(ka)\sum_{s=1}^{\infty} x_{2s}^{(N+1)/2} U_{2s} W_{m,2s}^{(p,(N+1)/2)} = 0, \tag{4}$$

EO (x –even; y -odd)

$$x_m^{(p)} - J_m(ka)\sum_{j=1}^{N/2}\sum_{s=0}^{\infty}\mu_s x_s^{(j)} U_s W_{ms}^{(p,j)} + 2J_m(ka)\sum_{s=0}^{\infty}\mu_s x_{2s}^{(N+1)/2} U_{2s} W_{m,2s}^{(p,(N+1)/2)} = 0, \tag{5}$$

OO (x –odd; y -odd)

$$x_m^{(p)} + J_m(ka)\sum_{j=1}^{N/2}\sum_{s=1}^{\infty} x_s^{(j)} U_s W_{ms}^{(p,j)} + 2J_m(ka)\sum_{s=1}^{\infty} x_{2s}^{(N+1)/2} U_{2s} W_{m,2s}^{(p,(N+1)/2)} = 0, \tag{6}$$

here $m = 1,\ldots N$, $p = 1,\ldots N/2$ if N is even and $p = 1,\ldots(N+1)/2$ if N is odd,

$$x_m^{(p)} = A_m^{(p)} F_m J_m(ka), \qquad U_{ms}^{(p,j)} = \frac{V_s}{F_s J_s(ka)},$$

$$W_{ms}^{(p,j)} = \begin{cases} \pm H_{m+s}^{(2)}((N-j)kh) \pm (-1)^s H_{m-s}^{(2)}((N-j)kh), & p = j, \\ H_{m-s}^{(2)}((j-p)kh) \pm (-1)^s H_{m\mp s}^{(2)}((j-p)kh) + \\ +(-1)^s H_{m-s}^{(2)}((N-j)kh) \pm H_{m\mp s}^{(2)}((N-j)kh), & p \neq j, \end{cases}$$

$$W_{ms}^{(p,(N+1)/2)} = H_{m-2s}^{(2)}(((N+1)/2-p)kh) \pm \pm H_{m+2s}^{(2)}(((N+1)/2-p)kh),$$

$$h = 2a + d.$$

In $W_{ms}^{(p,j)}$, we take the sign $"+"$ for the x -even SPs and $"-"$ for the x -odd SPs. We have to stress that last terms in (3)–(6) appear only for odd number of wires in a chain.

Finding the eigenvalues is equivalent to the computation of zeros of the determinants of derived matrix equations (3)–(6). They are the Fredholm second kind matrix equations and hence can be truncated so that approximate solution will converge to exact solution with increasing the truncation number. The necessary truncation number is determined by the wire radii, the distance between them, and the desired accuracy. This is because for more accurate description of the fields, higher-order multipole terms of (1), (2) should be taken into account for closely spaced wires. In this study the truncation number *N* = 20 of each of *N* x *N* blocks was used to provide the 10^{-4} accuracy.

Note that for distant wires with $d > a$ the influence of the higher-order series terms become negligibly small due to decaying character of the Hankel functions.

III. Numerical Results and Disscusion

Coupled dipole plasmons of a linear chain of nanowires are the symmetric and asymmetric combinations of plasmons of individual wires. Here, the coupled dipole plasmons with even symmetry fields with respect to both axes can be viewed as the transverse opposite-phase plasmons.

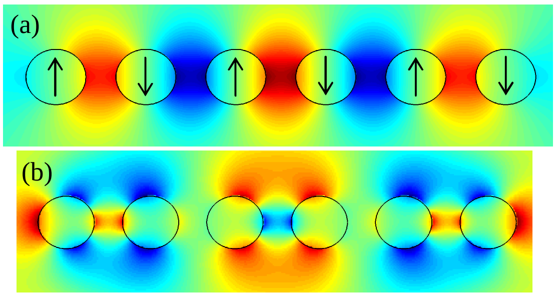

Fig. 3. The near-field patterns of (a) dipole and (b) quadrupole EE coupled localized SPs for six nanowires of a linear chain ($d = 20$ nm).

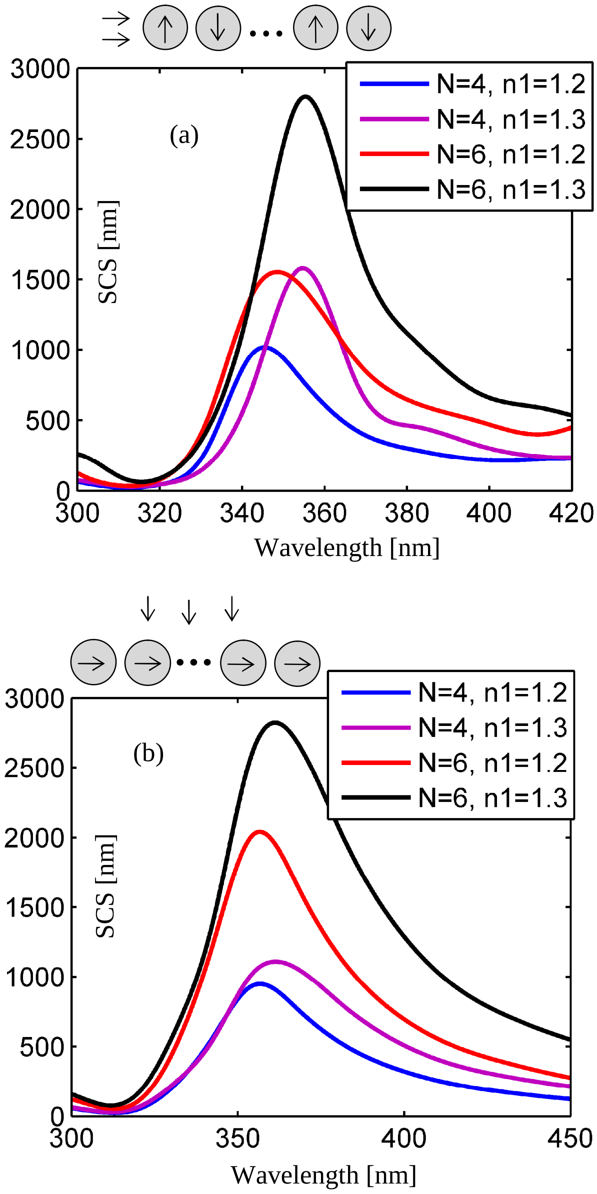

Fig. 4. The wavelength scans of SCS of coupled silver nanowires of a linear chain for different values of permittivity of environment ($d = 350$ nm).

Dipole EO plasmons are transversal in-phase ones, OE and OO are in-phase and opposite-phase longitudinal plasmons, respectively. Total number of coupled dipole plasmons in a finite linear chain of N nanowires equals to $2N$ (for details see [10]). Similar combinations of localized SPs exist in the coupled metal wires of a cluster with triangular or square configuration [10-13].

Among the possible coupled plasmons, there exist the plasmons with completely symmetrical fields with respect to all the axes of symmetry (EE). Fig. 3 presents near-field pattern for (a) dipole and (b) quadrupole EE coupled plasmons of six nanowires. The orientation of their dipole moments is shown in the insets.

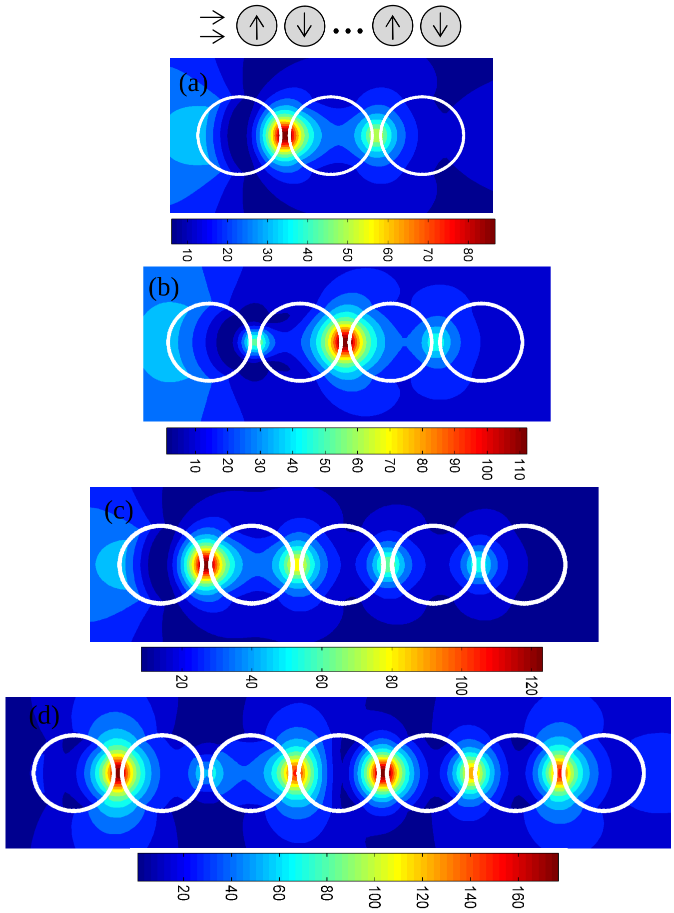

Fig. 5. The magnetic near-field of coupled silver nanowires of a linear chain for separation distance $d = 5$ nm ($n_1 = 1$): (a) $N = 3$, $\lambda = 340.5$ nm, (b) $N = 4$, $\lambda = 340.2$ nm, (c) $N = 5$, $\lambda = 340$ nm, (d) $N = 7$, $\lambda = 339$ nm.

Most of these plasmons are ‘dark’ ones that do not couple efficiently to an incident plane wave. Fig. 4 presents the scattering cross section (SCS) of a linear chain ($d = 320$ nm). Illumination direction is shown in the inset. In this case ‘bright’ plasmons are exited. For a linear chain, the ‘bright’ coupled plasmons are opposite-phase (EE) plasmons and longitudinal in-phase (OE) plasmons, and the ‘dark’ plasmons are transversal in-phase (EO) coupled plasmons and longitudinal opposite-phase (OO) plasmons. The shift in the resonance wavelength (λ) of the opposite-phase plasmon exceeds the corresponding value for the longitudinal in-phase plasmon and reaches a maximum when the separation distance between the wires is approximately equal to the wavelength.

The shift of the plasmon resonance of the opposite-phase plasmon is observable from $\lambda = 342$ nm to $\lambda = 351$ nm for four nanowires and from $\lambda = 345$ nm to $\lambda = 356$ nm for six nanowires while the refractive index of environment changes from $n_1 = 1.2$ to $n_1 = 1.3$ (see Fig. 4 (a)). The shift of the plasmon resonance of the longitudinal in-phase plasmon is observable from $\lambda = 353$ nm to $\lambda = 360$ nm for four nanowires and from $\lambda = 354$ nm to $\lambda = 363$ nm for six nanowires while the refractive index of environment changes from $n_1 = 1.2$ to $n_1 = 1.3$ (see Fig. 4 (b)).

In the gap between two or more nanowires, it is possible to obtain strong field concentration (hot spots) at the plasmon resonance wavelengths. Fig. 5 presents the magnetic near field patterns of coupled silver wires of a linear chain for the separation distance $d = 5$ nm. These field patterns reveal the opposite-phase plasmons. We see that with increasing of wires number the amplitude of the electromagnetic field in hot spots increases, while the position of strong concentration area depends on the number of wires in the chain.

Fig. 6 shows the scattered magnetic far-field angular patterns of coupled silver nanowires of a linear chain for the separation distances $d = 100$ nm and $d = 350$ nm. The frequency of the incident field coincides with the corresponding plasmon resonance frequency. The direction of the plane wave is shown in the inset. With increasing the number of wires, the scattered field collimation occurs in a narrow shadow beam, and a decrease of the separation distance lowers the side and rear lobes.

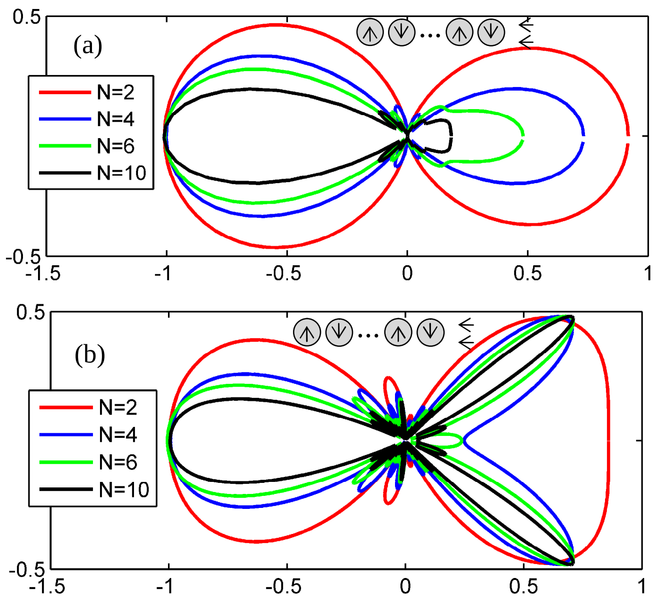

Fig. 6. The scattered magnetic far-field angular patterns of coupled silver nanowires of a linear chain ($n_1 = 1$): (a) $d = 100$ nm and (b) $d = 350$ nm.

Conclusions

The plasmonic properties of the coupled silver nanowires arranged in finite linear chain have been analyzed. Hybrid plasmonic modes of the coupled silver nanowires of such configurations have been studied. Maximum shift of the plasmon resonance peak in the SCS is observable for the excitation of the opposite-phase coupled plasmons of silver nanowires. It was found that, in a linear chain of silver nanowires, the opposite-phase coupled plasmons have the maximum sensitivity to the changes in the refractive index of the environment, and this sensitivity increases with the number of wires in a finite linear chain.

References

[1] A. Zayats and I. Smolyaninov, "Near-field photonics: Surface plasmon polaritons and localized surface plasmons," J. Opt. A, Pure App. Opt., vol. 5, pp. 16–50, 2003.

[2] N. Bonod, A. Devilez, B. Rolly, S. Bidault, and B. Stout, "Ultracompact and unidirectional metallic antennas," Phys.Rev. B, vol. 82, 115429, 2010.

[3] P. Jonson and R. Christy, "Optical constants of the noble metals," Phys. Rev. B, vol. 6, pp. 4370-4379, 1972.

[4] D. Natarov, V. Byelobrov, R. Sauleau, T. Benson, and A. Nosich, "Periodicity – induced effects in the scattering and absorption of light by infinite and finite gratings of circular silver nanowires," Opt. Exp., vol. 19, no 22, pp. 22176-22190, 2011.

[5] J. Anker, W. P. Hall, O. Lyandres, N. Shan, J. Zhao and R. Van Duyne, "Biosensing with plasmonic nanosensors," Nature Materials, vol. 7, pp. 442-453, 2008.

[6] D. Fedyanin and A. Arsenin, "Transmission of surface plasmon polaritons through a nanowire array: Mechanooptical modulation and motion sensing," Opt. Exp., vol. 18, no. 19, pp. 20115–20124, 2010.

[7] M. Noginov, G. Zhu, A. Belgrave, R. Bakker, V. Shalaev, E. Narimanov, S. Stout, E. Herz, T. Suteewong, and U. Wiesner, "Demonstration of a spaser-based nanolaser," Nature, vol. 460, pp. 1110–1113, 2009.

[8] D.M. Natarov, "Modes of a core-shell silver wire plasmonic nanolaser beyond the Drude formula," IOP J. Opt., vol. 16, no 7, pp. 075002/6, 2014.

[9] E. Smotrova, A. Nosich, T. Benson, and P. Sewell, "Optical coupling of whispering-gallery modes of two identical microdisks and its effect on photonic molecule lasing," IEEE J. Select. Topics Quant. Electron., vol. 12, pp. 78-85, 2006.

[10] E.I. Smotrova, A.I. Nosich, T.M. Benson, and P. Sewell, "Threshold reduction in a cyclic photonic molecule laser composed of identical microdisks with whispering-gallery modes," Opt. Lett., vol. 31, no 7, pp. 921-923, 2006.

[11] S.V. Boriskina, et al., "Directional emission, increased free spectral range, and mode Q-factors of 2-D wavelength-scale optical microcavity structures," IEEE J. Select. Topics Quant. Electron., vol. 12, no 6, pp. 1175-1182, 2006.

[12] N. Stognii and N. Sakhnenko, "Plasmon resonances and their quality factors in a finite linear chain of coupled metal wires," IEEE J. Select. Topics Quant. Electron., vol. 19, No. 3, art no 4602207, 2013.

[13] N.P. Stognii and N.K. Sakhnenko, "Plasmonic properties of coupled metal wires in the cluster with triangular or square configuration," Proc. In Conf. Electron. Nanotechnol. (ELNANO-2015), pp. 112-115, Kiev, 2015.